Influence of an external electric field on cAMP wave patterns in aggregating Dictyostelium discoideum

Jiří Lindner,[1] Hana Ševčíková[2,*] and Miloš Marek[1,2]
[1]*Department of Chemical Engineering, Institute of Chemical Technology, Technická 5, 166 28 Prague 6, Czech Republic*
[2]*Center for Nonlinear Dynamics of Chemical and Biological Systems, Institute of Chemical Technology, Technická 5, 166 28 Prague 6, Czech Republic*

(Received 13 October 2000; revised manuscript received 4 December 2000; published 23 March 2001)

Effects of an external electric field on the propagation of excitable cyclic adenosin monophosphate (cAMP) pulses in aggregating cells of Dictyostelium discoideum have been studied by means of numerical simulations. The mathematical model includes a three-variable version of the Martiel-Goldbeter kinetic model of cAMP production by cells, and diffusion and electromigration of cAMP through intercellular space. Electric field effects on the planar pulses propagating in a spatially one-dimensional system and on circular and spiral pulses propagating in a spatially two-dimensional system include changes in the propagation velocities of pulses initiated in the field-free system, the annihilation of pulses propagating towards the cathode by electric fields of high intensities, and the formation of region(s) of spontaneous excitation permanently generating trains of cAMP pulses. The spiral patterns were found to drift in the electric fields of low intensities, fields of high intensities were found to decompose the spiral arms on the side facing the negative electrode.

DOI: 10.1103/PhysRevE.63.041904 PACS number(s): 87.50.Rr, 87.18.Hf, 87.18.Bb, 87.18.Pj

I. INTRODUCTION

A layer of aggregating cells of a slime mold Dictyostelium discoideum (DD) represents an excitable medium [1–3] through which pulses of increased concentration of cyclic adenosin monophosphate (cAMP) propagate in the form of either circular or spiral wave patterns [4,5]. Pulses are emitted when the environment lacks nutrients and their functions are (i) to transmit information on adverse living conditions from cell to cell and (ii) to create a traveling gradient of chemoattractant (cAMP) against which the cells move towards the centers where they aggregate and develop into fruiting bodies enabling the organism to survive [6].

Propagation of cAMP pulses in DD have been intensively studied for they represent a vehicle of cell to cell communication and, in DD itself, are assumed to play an important role in the development of the originally unicellular form of the organism into a highly spatially organized multicellular form [7–9]. The propagation of cAMP pulses through the randomly distributed DD cells begins when the environment becomes depleted of nutrients. Some of the starving cells begin to produce cAMP periodically which is then excreted into the intercellular space and diffuses to their neighboring cells. These respond to the arriving pulse of the increased cAMP concentration by producing more of it autocatalytically and excreting it into the neighborhood. As a result the pulse of the increased cAMP concentration is relayed through the cell layer. Cells prolongate and move up the cAMP gradient towards the source of the pulse of increased cAMP concentration. After about 50 pulses all the neighboring cells gather, forming a mound, and the further development of DD from a single-cell culture to a multicellular organism starts. About 10^5 cells need to gather in order to develop into a fruiting body [9].

The mechanism for the propagation of cAMP pulse waves [10]—the interaction of a local transformation process (autocatalytic biochemical reaction in this case) with a spatially oriented process (diffusive transport in this case)—is a general mechanism underlying the propagation of pulse waves in diverse excitable media [11] such as homogeneous chemical reacting mixtures [12], the yeast extract [13], the neuron axons [14], and the heart muscle [15]. As biochemical media often consist of ionic species the propagation of pulse waves, and a variety of dynamical modes of wave patterns, can be controlled by applying an external electric field. This selectively affects the spatial process by adding the electromigration transport of ionic species to their diffusional spreading [16].

The effects of an external electric field on pulse waves have been widely studied in the chemical excitable system—formed by the Belousov-Zhabotinski (BZ) reaction medium—both experimentally and by means of mathematical modelling [16–21]. The effects include both the decrease and increase of the pulse propagation velocity, annihilation of the pulse, breaking of continuous circular pulses into fragments, enhancement (or suppression) of spiral wave formation, the drift of spiral centers through the system, and phenomena resulting from a modified refractoriness of the medium, namely the reversal of the direction of the pulse propagation and pulse splitting (i.e., the back firing of new pulses from the back of the existing one).

We have previously studied the effects of external electric fields on propagation of pulse waves in two mathematical models of excitable media [22]. One of the models was based on the FitzHugh-Nagumo equations which describe the transmission of an action potential along a nerve fiber [23] and is often used as a general model of excitable systems. The second model employed the Martiel-Goldbeter re-

*E-mail address: hana.sevcikova@vscht.cz

action mechanism [6,24] for cAMP production in DD cells equipped with a genetic feedback [25]. We found that the external electric field causes variations in the propagation velocity, annihilation of pulses, fragmentation of a continuous pulse, and formation of spirals. However, we failed in simulating the phenomena related to the changes in the system refractoriness—pulse reversal and splitting.

In this paper we attempt to simulate the reversal and splitting of cAMP pulses using the three-variable Martiel-Goldbeter model of cAMP production [24,26]. Parameters of the model were chosen both to match physiologically meaningful values and to support the excitable dynamic regime in the kinetic model. The effects of an external electric field were investigated on planar pulse waves propagating in a spatially 1D system and on circular and spiral waves propagating in a spatially 2D system.

II. MATHEMATICAL MODEL

A. Kinetics of the cAMP production

The kinetics of the cAMP production in DD cells are described by the Martiel-Goldbeter model [24] which is based on the desensitization of cAMP receptors on the cell membrane. In the model, extracellular cAMP binds to cell receptors and the receptor-cAMP complex activates the enzyme adenylate cyclase inside the cell which produces intracellular cAMP from ATP (adenosin triphosphate). The intracellular cAMP is excreted to the extracellular space where it binds to available receptors on the cell membrane. This positive feedback loop ensures the fast rise of the extracellular cAMP concentration which, later on, causes the desensitization of receptors. The active state of receptors is recovered after the extracellular enzyme—phosphodiesterase—hydrolyzes the extracellular cAMP. The three-variable version of the kinetic model is given by the following set of ordinary differential equations

$$r_\beta = \frac{d\beta}{dt} = q\sigma\Phi(\rho_T,\gamma,\alpha) - (k_i + k_t)\beta, \tag{1}$$

$$r_\gamma = \frac{d\gamma}{dt} = \frac{k_t}{h}\beta - k_e\gamma, \tag{2}$$

$$r_{\rho_T} = \frac{d\rho_T}{dt} = -f_1(\gamma)\rho_T + f_2(\gamma)(1-\rho_T), \tag{3}$$

with

$$f_1(\gamma) = (k_1 + k_2\gamma)/(1+\gamma),$$

$$f_2(\gamma) = (k_1 L_1 + k_2 L_2 c\gamma)/(1+c\gamma),$$

$$\Phi(\rho_T,\gamma,\alpha) = \alpha(\lambda\theta + \varepsilon Y^2)/[1 + \alpha\theta + \varepsilon Y^2(1+\alpha)],$$

$$Y = \rho_T\gamma/(1+\gamma).$$

In the above, β and γ denote concentrations of intracellular and extracellular cAMP, respectively, divided by the dissociation constant K_R of the cAMP-receptor complex in an active state ($K_R = 10^{-7}$ M); ρ_T denotes the fraction of receptors in the active state.

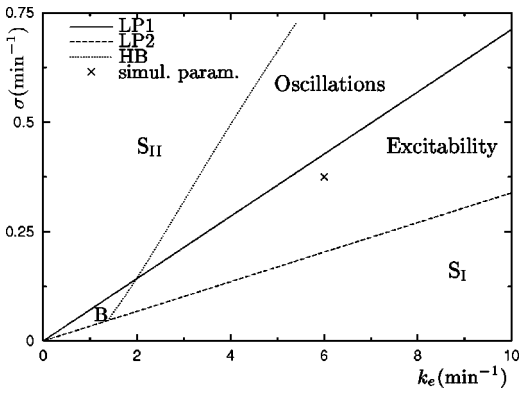

FIG. 1. Bifurcation diagram of the system described by Eqs. (1)–(3) in the parametric plane σ–k_e, see Ref. [26]. For the parameters of the model, see text. S_I (S_{II}): regions of the existence of a single stable stationary state with low (high) concentrations of extracellular (γ) and intracellular (β) cAMP and high (low) concentration of active receptors (ρ_T). B: bistable region; LP1 and LP2: limit points on S_I and S_{II} stationary solution branches, respectively; HB: Hopf bifurcation on the S_{II} stationary solution branch. × denotes the characteristic point for which the numerical simulations were performed ($\sigma = 0.375$, $k_e = 6.0$, concentrations in the stable stationary state: $\gamma_{ss} = 0.00696$, $\beta_{ss} = 0.232$, $\rho_{T,ss} = 0.893$).

The values of model parameters used in the simulations are $c = 10$, $h = 5$, $k_1 = 0.09\ \mathrm{min}^{-1}$, $k_2 = 1.665\ \mathrm{min}^{-1}$, $k_i = 1.7\ \mathrm{min}^{-1}$, $k_e = 6.00\ \mathrm{min}^{-1}$, $k_t = 0.9\ \mathrm{min}^{-1}$, $L_1 = 10$, $L_2 = 0.005$, $q = 4000$, $\varepsilon = 1$, $\lambda = 0.01$, $\sigma = 0.375\ \mathrm{min}^{-1}$, $\theta = 0.01$, $\alpha = 3$. The parameter values used result from the experimental values listed in Tables I and II in Ref. [24], except for values of k_1 and k_2 which were multiplied by a factor of 2.5 in order to obtain a better agreement between experimental and calculated values of the period of the pulse waves [26].

Parameters σ and k_e are the main parameters governing the dynamic modes of the kinetic model described by Eqs. (1)–(3) [26] as can be seen in Fig. 1. The parameter σ corresponds to the maximum activity of adenylate cyclase, the enzyme producing the intracellular cAMP after being activated by an active cAMP-receptor complex, and k_e is the rate constant of degradation of extracellular cAMP by extracellular phosphodiesterase. This parameter thus controls the recovery of receptors to their active state.

B. Spatially distributed systems

The model of spatially one- and two-dimensional systems (formed by a layer of DD cells) is based on the molar balance equations of the three system components considered in Eqs. (1)–(3). The model is derived assuming a homogeneous layer of cells in the early stages of the cell aggregation. The changes in the cell density due to their chemotaxis are omitted since the velocity of cell motion is 10 times slower than the velocity of cAMP pulses propagation [9]. As a consequence, the changes of both the receptor and intracellular

cAMP concentrations occur only due to reaction. On the contrary, extracellular cAMP flows through the intercellular space by both molecular diffusion and migration in the gradient of externally applied electric potential. The spatially 2D form of the reaction-diffusion-migration model then reads

$$\frac{\partial c_\beta}{\partial t} = r_\beta, \tag{4}$$

$$\frac{\partial c_\gamma}{\partial t} = r_\gamma + D_\gamma\left(\frac{\partial^2 c_\gamma}{\partial x^2} + \frac{\partial^2 c_\gamma}{\partial y^2}\right) - z_\gamma D_\gamma \frac{F}{RT}\left(e_x \frac{\partial c_\gamma}{\partial x} + e_y \frac{\partial c_\gamma}{\partial y}\right), \tag{5}$$

$$\frac{\partial c_{\rho_T}}{\partial t} = r_{\rho_T}. \tag{6}$$

In Eqs. (4)–(6) c_i represents the concentration of the ith component ($i=\beta,\gamma,\rho_T$), r_i its source by biochemical reaction, D_γ is diffusion coefficient of cAMP ($D_{\mathrm{cAMP}} = 0.024$ mm^2 min^{-1} [10]), z_γ its electric charge (we assume $z_{\mathrm{cAMP}} = -1$), x and y are space co-ordinates, t is time, e_x and e_y the (constant) intensity of the electric field in the x and y directions; $F = 96485$ C mol^{-1} and $R = 8.314$ J mol^{-1} K^{-1} are the Faraday and universal gas constants, and $T = 294.15$ K (21 °C) is temperature. The value of T corresponds to the temperature at which the experimental studies of DD cells aggregation are usually performed. The source terms r_i are defined by Eqs. (1)–(3). For a spatially 1D system $\partial c_\gamma/\partial y = \partial^2 c_\gamma/\partial y^2 = 0$.

C. Simulation procedure

To perform the bifurcation analysis of the kinetic equations (1)–(3) the continuation software package CONT [27] has been used. Dynamic simulations of kinetic equations (1)–(3) have been carried out with a FORTRAN code, which utilizes the Merson modification of the Runge-Kutta method with the automatic regulation of the time step.

The set of partial differential equations (4)–(6) was solved by the method of lines. The spatial derivatives were approximated by three-point differences on an equidistant grid of $N_x \times N_y$ points. Zero-flux boundary conditions were used. The resulting system of $3 \times N_x \times N_y$ ordinary differential equations was integrated by the Merson modification of the Runge-Kutta method.

The simulations of cAMP propagation in the spatially 1D system were performed on a system of length 25 mm with $N_x = 501$ and $N_y = 1$. The spatially 2D simulations were carried out both on a rectangular area with length (x coordinate) 50 mm and width (y coordinate) 10 mm divided into $N_x = 1001$ and $N_y = 201$ spatial points and on a square area 25 $\times$ 25 mm with $N_x = N_y = 501$ spatial points.

In simulations, the electric field is oriented along the x axis ($e_x \neq 0, e_y = 0$) and only positive values of e_x were applied. The electric field was always applied on the already traveling pulse and was kept constant. The convention used throughout means that the anode is placed on the left side of the system while the cathode is placed on the right side.

III. RESULTS OF NUMERICAL SIMULATIONS

A. Analysis of the kinetic model and dynamical simulations in CSTR

The bifurcation diagram of the kinetic equations (1)–(3) is shown in Fig. 1. The region of excitability is characterized by the existence of three stationary states of Eqs. (1)–(3), one of them (with low values of β and γ and high value of ρ_T) being stable.

The excitable behavior in a CSTR (lumped parameter system) was examined first. The excitable response is observed for values of $\gamma_{\mathrm{per}} \geqslant 6 \cdot \gamma_{ss}$ and higher. Slightly above the threshold value of γ_{per} a delayed response of the system to the perturbation is observed; when $\gamma_{\mathrm{per}} \leqslant 5 \cdot \gamma_{ss}$ the system returns quickly to the initial stable steady state without moving along the excitation cycle.

The superthreshold perturbation of the extracellular cAMP concentration (γ) initiates the autocatalytic production of the intracellular cAMP (β) followed closely by the fast increase of the extracellular cAMP concentration. The consequent decrease of the concentration of active receptors (ρ_T), due to binding the extracellular cAMP and desensitization, results in the cessation of the intracellular cAMP production followed by the decrease of the extracellular cAMP concentration due to its dephosphorylation. Consequently, the active state of receptors is recovered and the system returns to the initial stable stationary state.

B. Spatially 1D dynamical simulations

When a superthreshold perturbation of γ is applied in the small central region of the spatially distributed one-dimensional system (Fig. 2, $t = 0$ min) the whole region undergoes an excitation cycle giving birth to two identical pulses propagating outwards from the center (Fig. 2, $t = 2$ and 5 min). After a weak constant electric field is applied the amplitude and velocity of the cAMP pulse propagating towards the anode (to the left) increases while the cAMP pulse propagating in the opposite direction reduces both its amplitude and propagation velocity (Fig. 2, $t = 25$ min). After the two pulses have passed through the system the initial, spatially homogeneous steady state is restored.

Figure 3 shows the concentration profiles of all three system components. It can be seen that the concentration changes in γ follow closely the changes in β and that return of ρ_T to the steady state is significantly slower than the return of either γ or β.

When a slightly stronger electric field ($e_x = 1.25$ V/cm) is applied on a pair of traveling pulses a spontaneous excitation occurs in the small region behind the pulse propagating towards the cathode as shown in Fig. 4 ($t = 18$ and 19 min). Two pulses of cAMP are formed in this region ($t = 20$ min) and propagate outwards ($t = 22$ min). The maximum concentration of γ in the pulse propagating towards the anode (to the left) is higher than that of the pulse propagating to the cathode. Another excitation occurs at $t = 34$ min in the

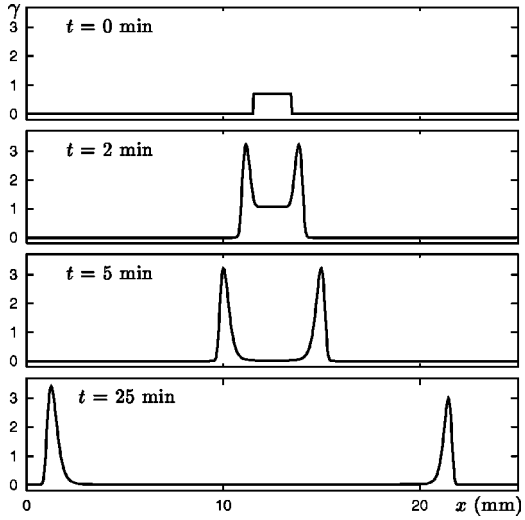

FIG. 2. Effects of a weak electric field on propagation of cAMP pulses. At time $t=0$ min the steady state values β_{ss}, γ_{ss}, and $\rho_{T,ss}$ were used as the spatially homogeneous initial conditions and the superthreshold perturbation of γ ($\gamma_{\mathrm{per}}=10^2\cdot\gamma_{ss}$) has been applied in the centre of the system. At time $t=5$ min the electric field 1 V/cm was switched on.

small region behind the new right-propagating pulse giving again birth to two new pulses. This process repeats periodically and as a result two pulse trains propagating in the opposite directions arise in the system. The wavelength of the right periodic train is much shorter than that of the left propagating train as is the propagation velocity and the amplitude of pulses. The periods between consequent pulses are much longer in the left train than in the right one. The region of spontaneous excitations propagates towards the cathode as can be seen in the space-time plot in Fig. 5. The spontaneous excitation occurs while the region is still in the refractory state, not fully recovered from the preceding excitation.

The interference of the pulses emitted asynchronously from two excitation regions (marked by dotted and dashed lines) formed behind the pulse propagating to the cathode takes place when an electric field of intensity 2 V/cm is switched on (see Fig. 5). Each excitation gives rise to two

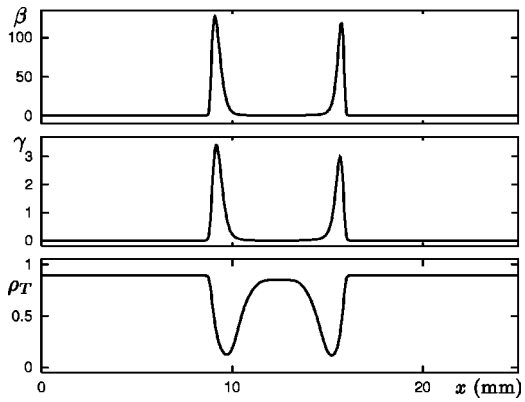

FIG. 3. Comparison of spatial profiles of β (top), γ (middle), and ρ_T (bottom) at time 7 min (i.e., 2 min after switching the electric field on), $e_x=1$ V/cm.

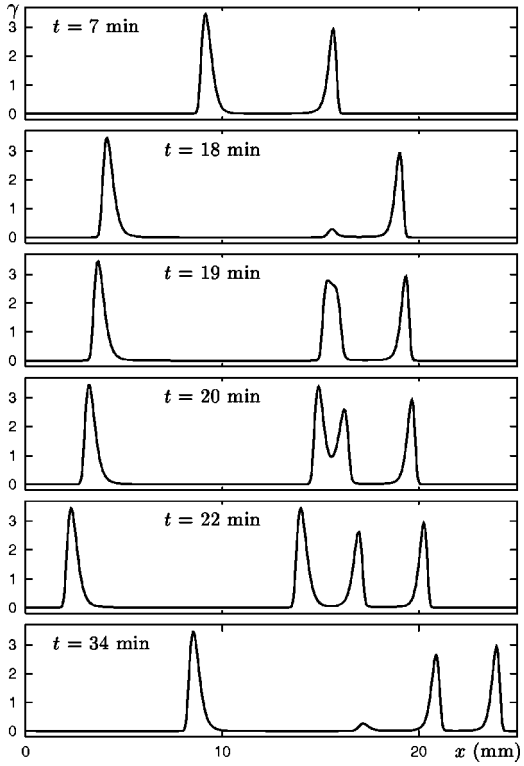

FIG. 4. Spontaneous excitation of cAMP pulses by the electric field of the intensity $e_x=1.25$ V/cm (switched on at $t=5$ min). Spatial profiles of extracellular cAMP concentration (γ) are shown.

pulses propagating outwards from the excitation regions. Two of the four pulses that propagate towards each other mutually annihilate and thus only two pulses remain propagating in the opposite directions, towards the ends of the system. The process repeats periodically giving rise to two pulse trains differing considerably in their amplitudes, velocities, wavelength, and periods. The left region of spontaneous excitation is almost stationary while the right region slowly moves towards the cathode.

As the intensity of the applied electric field increases from $e_x=1.25$ V/cm to 2 V/cm (see Fig. 5) the wavelengths of both the left and the right pulse trains decrease, the wavelength of the left train being always longer than that of the right one. The propagation of the left train (propagating towards the anode) speeds up with increasing field intensity while the propagation of the right train slows down thus increasing the difference between the velocities of the left and right trains. The difference in amplitudes of the left and right pulses also increases with increasing field intensity and more profound effects are seen on the right propagating pulses. Periods of both trains decrease with the increasing field intensity with periods of the left wave train being higher than the periods of the right trains.

The differences mentioned above develop further when the electric field intensity is increased until the amplitude of the right propagating pulses gets very small and the pulses obtain the form of attenuating rippling at $e_x=4$ V/cm as illustrated in the space-time plot in Fig. 5. A region of spontaneous excitation also forms behind the right propagating pulse when an even stronger field ($e_x=6$ V/cm) is applied.

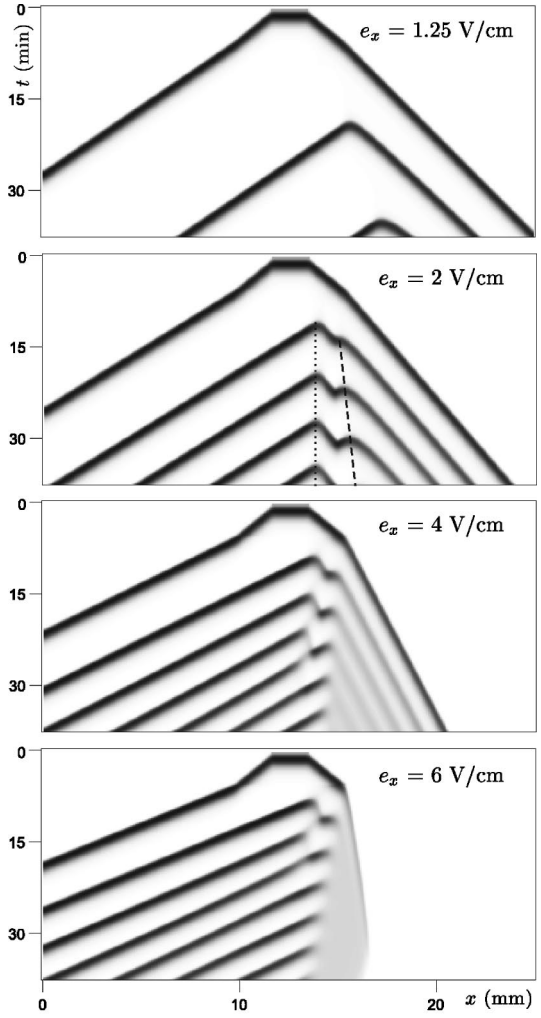

FIG. 5. Space-time plots of the spontaneous excitation of cAMP pulses by electric fields of different intensities. Grey-scale corresponds to the extracellular cAMP concentration (black: the maximal concentration of γ). Dotted and dashed lines trace the positions of two regions of spontaneous excitation.

However, in this field, only the left propagating pulses are emitted from this region. The amplitude of the left propagating pulses was observed to decrease with each newly emitted pulse until an almost constant value was reached at $t=45$ min. Later ($t=95$ min) the amplitude of the pulses, and also the wavelength of the pulse train, increased again. The region of spontaneous excitation propagates slowly towards the anode. The original right propagating pulse abruptly diminishes both in its amplitude and velocity of propagation after the electric field is switched on and, after a short time, ceases to exist as can be seen in the space-time plot in Fig. 5.

C. Spatially 2D dynamical simulations

The effects of an applied electric field on a circular pulse of cAMP propagating in a spatially 2D system are illustrated in Figs. 7, 8, and 9. The circular wave was initiated at time $t=0$ by increasing the value of γ from its steady state value to the perturbation value $\gamma_{\mathrm{per}}=10^2\times\gamma_{ss}$ in the circular region (see Fig. 6). After some time a circular pulse wave develops propagating symmetrically outwards from the perturbed region (see Fig. 7, $t=5$ min).

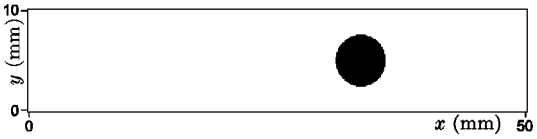

FIG. 6. Initial perturbation of the extracellular cAMP concentration (γ) in 2D simulations. Superthreshold perturbation of γ (γ_{per}, denoted by black, $=10^2\times\gamma_{ss}$, denoted by white) was applied on the circular area (diameter 5 mm) in the center of the system.

The effects of an electric field of $e_x=1.5$ V/cm are illustrated in Fig. 7. After the electric field is switched on at time $t=5$ min a region of spontaneous excitations is established close behind the right propagating arc ($t=15$ min) repeatedly giving rise to elipsoidlike pulse trains. The train of pulses propagating towards the cathode has both a shorter wavelength and lower amplitude than the train of pulses propagating to the anode. In general, the effects of the electric field of intensity 1.5 V/cm on the circular pulse in 2D system correspond to the effects of an electric field of intensity 1.5 V/cm on pulses propagating in the spatially 1D system.

A region, in which new cAMP pulses are spontaneously generated, is also established behind the right arc of the first circular wave when an electric field of intensity 3.8 V/cm is applied (see. Fig. 8). The pulses propagating to the right are of very low amplitudes (see Fig. 8, $t=49$ min) forming a rippling rather than a pulse train. Pulses propagating to the left have quite large amplitudes and we can observe that the initially waved-shaped pulses smooth out during the propagation, most likely due to the curvature dependence of the

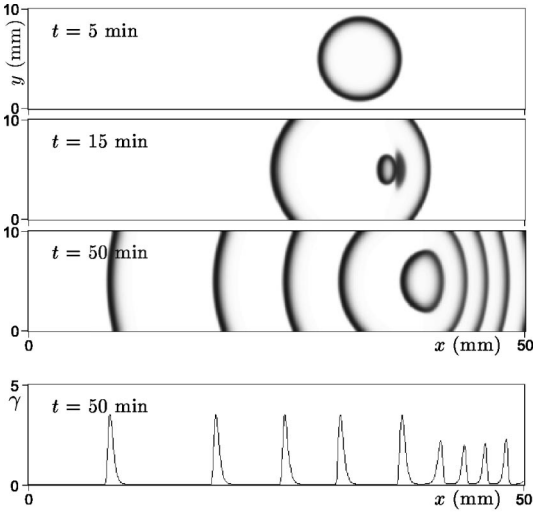

FIG. 7. Spontaneous excitation of cAMP pulses in the imposed electric field. Spatial profiles of extracellular cAMP concentration (γ) are shown in the gray scale. The bottom figure shows a spatial profile of cAMP concentration along the line $y=5$ mm. At time $t=5$ min the electric field of the intensity $e_x=1.5$ V/cm, $e_y=0$ was switched on.

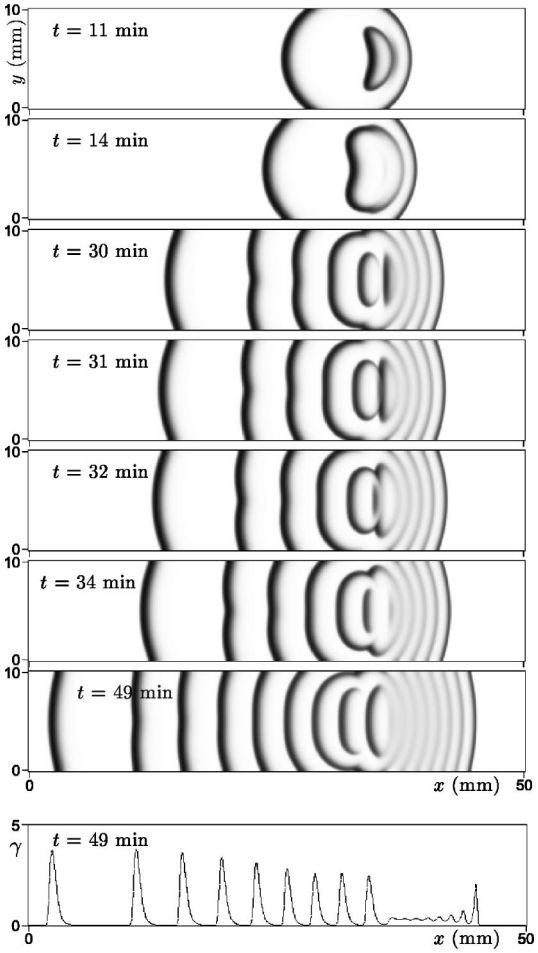

FIG. 8. Spontaneous generation of the train of cAMP pulses, formation of rippling pulses, and interference of the cAMP pulses occurring after the electric field of the intensity $e_x=3.8$ V/cm, $e_y=0$ is switched on at time $t=5$ min, 2D simulations. The spatial distribution of extracellular cAMP concentration (γ) is shown utilizing the gray scale. The bottom figure shows a spatial profile of cAMP concentration along the line $y=5$ mm.

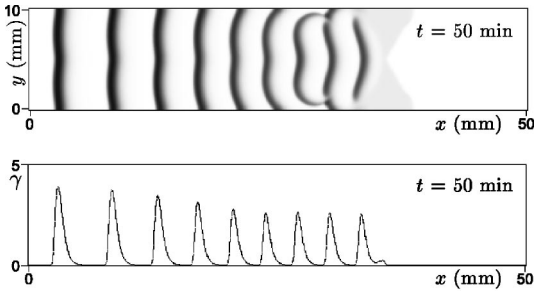

FIG. 9. Annihilation of the right pulse train of the cAMP concentration pulses in a strong electric field (intensity $e_x=6.1$ V/cm, $e_y=0$) switched on at time $t=5$ min. 2D simulations. Spatial profiles of extracellular cAMP concentration (γ) are shown utilizing the gray scale. The bottom figure shows the spatial profile of γ taken at $t=50$ min and $y=5$ mm.

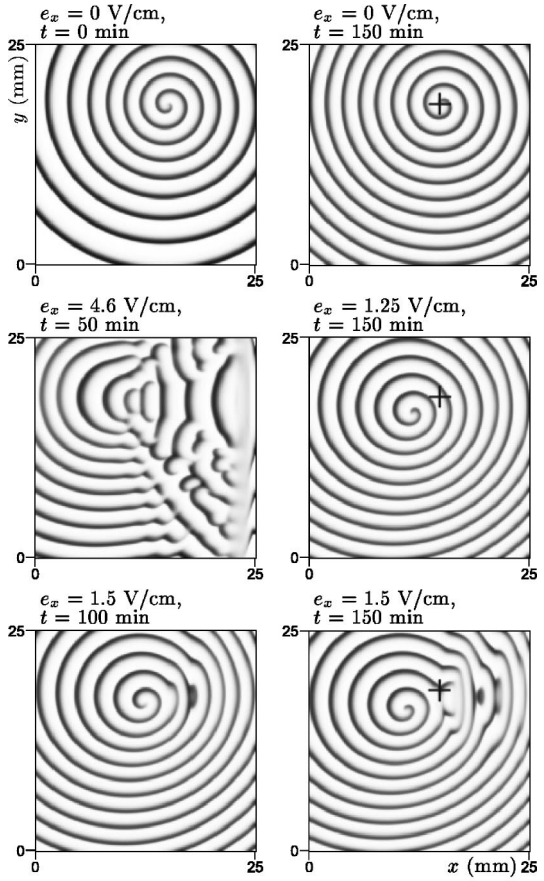

FIG. 10. Influence of electric fields of different intensities on the extracellular cAMP concentration (γ) spiral pulses. + denotes the position of the spiral tip at $e_x=0$ V/cm, $t=0$ min.

propagation velocity. Notice also that from time $t=30$ min almost planar pulse fragments propagating to the left are generated. Their free ends curve and later interfere with the following pulse fragment.

Effects of an electric field of intensity 6.1 V/cm cause the annihilation of the pulse arc propagating to the right and only one periodic wave train is generated propagating to the left (see Fig. 9) in analogy to what has been observed in the spatially 1D case for $e_x=6$ V/cm (see Fig. 5).

Effects of electric fields of various intensities on a spiral wave are illustrated in Fig. 10. A spiral develops spontaneously from a fragment of the pulse formed from the initial perturbation. Without an electric field, the spiral rotates with the spiral tip being fixed at a certain position ($e_x=0$, $t=150$ min); applied electric fields ($e_x=1.25$ V/cm, $e_x=1.5$ V/cm) cause the spiral tip to drift and shift in both the x and y directions. Higher electric field strengths evoke spontaneous excitations behind the spiral arms propagating to the right ($e_x=1.5$ V/cm, $t=100$ min) and the newly initiated pulse fragments interfere with already existing spiral arms ($e_x=1.5$ V/cm, $t=150$ min). The extensive decomposition of the right part of the spiral occurs when a high electric field ($e_x=4.6$ V/cm, $t=50$ min) is applied to the spiral.

IV. CONCLUSIONS

The numerical simulations described above revealed a wide variety of effects that an imposed dc electric field can have on cAMP pulses propagating in the homogeneous layer of aggregating DD cells. The effects include (i) changes in propagation velocities of pulses from those excited in the electric field-free system, (ii) the annihilation of pulses propagating towards the cathode by electric fields of high intensities, and (iii) the formation of regions of spontaneous excitations permanently generating trains of pulses.

Assuming the propagation of cAMP pulses mediates the aggregation of DD cells the results of the present study suggest that the imposed electric field can have profound effects on the aggregation process itself and, consequently, on the formation of mounds and the further development of DD into a multicellular organism. To verify this hypothesis both an experimental research and numerical simulations (based on the present mathematical model extended by the equation for the changes of the cell density [8,28–30]) of electric field effects on aggregation of DD cells is in progress.

The study shows that the imposed electric field can substantially increase the variety of dynamical modes of pulse waves propagation in excitable media. Comparing the effects of external electric fields on pulses of cAMP, propagating in the biochemical excitable system, with the effects an electric field has on pulse waves propagating in a chemical excitable system (the BZ medium [17,20,21]) we notice both analogies and differences between the two cases. The analogies include the speeding up of the pulses propagating towards the electrode that facilitates the flow of the autocatalyst from the pulse into the medium ahead of it and the slowing down of the pulses propagating in the opposite directions. The analogies also include the annihilation of pulses by high intensity electric fields.

The differences are found when the spontaneous generation of new pulses by an imposed electric field is considered. In the model of cAMP pulses a region (or regions) of spontaneous excitation arises behind the initial propagating pulse giving rise to two new pulses propagating outwards from this region. The excitation activity is permanent and, as a result, two permanent trains of pulses propagating in opposite directions are generated. The spontaneous generation of pulses is observed in a large interval of electric field intensities. When the intensity of an electric field becomes sufficiently large only the train propagating towards the anode is generated.

In the BZ system, the phenomenon called splitting resembles somewhat the spontaneous generation of trains of cAMP pulses. During the splitting, new pulses are fired from the back of the already existing pulse when an electric field is switched on. Only one train of pulses is formed propagating in the opposite direction to that of the ''mother'' pulse. The number of pulses in the train depends on the intensity of the electric field and permanent pulse trains were found only in a small interval of electric field intensities.

Contrary to the BZ system, where new pulses can split off only while the ''mother'' pulse exists, the train of cAMP pulses persists even after the electric field annihilates the original pulse behind which the region of spontaneous excitation has developed. Another difference resides in the fact that the reversal of cAMP pulses by the imposed electric field was not found as it was in the BZ pulses.

The direction of the spiral tip drift and shift is the same as in the case of BZ spirals; i.e., the spiral tip drifts in the direction parallel to the electric field towards the electrode causing pulses to accelerate; the shift of the spiral tip in the direction perpendicular to the electric field vector depends on the chirality of the spiral [18].

ACKNOWLEDGMENTS

This work was supported by the Ministry of Education, Czech Republic (Grant No. VS96073) and by the Grant Agency of the Czech Republic (Grant No. 203/98/1304).

[1] *Nonlinear Wave Processes in Excitable Media*, edited by A. V. Holden, M. Markus and H. G. Othmer (Plenum Press, New York, 1989).
[2] J. D. Murray, *Mathematical Biology* (Springer-Verlag, Berlin, 1989).
[3] J. Keener and J. Sneyd, *Mathematical Physiology* (Springer-Verlag, Berlin, 1998).
[4] K. J. Tomchik and P. Devreotes, Science **212**, 443 (1988).
[5] F. Alcantara and M. Monk, J. Gen. Microbiol. **85**, 321 (1974).
[6] A. Goldbeter, *Biochemical Oscillations and Cellular Rhythms* (Cambridge University Press, Cambridge, 1996).
[7] The Dictyostelium Virtual Library at URL http://dicty.cmb.nwu.edu/Dicty/dicty.html
[8] D. Dormann, B. Vasiev, and C. J. Weijer, Biophys. Chem. **72**, 21 (1998).
[9] P. Devreotes, Science **245**, 1054 (1984).
[10] J. J. Tyson, K. A. Alexander, V. S. Manoranjan, and J. D. Murray, Physica D **34**, 193 (1989).
[11] B. M. Sager, Genes Dev. **10**, 2237 (1996).
[12] A. N. Zaikin and A. M. Zhabotinski, Nature (London) **225**, 535 (1970).
[13] S. C. Müller, T. Mair, and O. Steinbock, Biophys. Chem. **72**, 37 (1998).
[14] A. L. Hodgkin and A. F. Huxley, J. Physiol. (London) **117**, 500 (1952).
[15] J. M. Davidenko, A. V. Pertsov, R. Salomonsz, W. Baxter, and J. Jalife, Nature (London) **355**, 349 (1992).
[16] P. J. Ortoleva, *Nonlinear Chemical Waves* (Wiley, New York, 1992).
[17] H. Ševčíková and M. Marek, Physica D **9**, 149 (1983).
[18] O. Steinbock, J. Schütze, and S. C. Müller, Phys. Rev. Lett. **68**, 248 (1992).
[19] J. J. Taboada, A. P. Muñuzuri, V. Pérez-Muñuzuri, M. Gómez-Gesteira, and V. Pérez-Villar, Chaos **4**, 519 (1994).
[20] J. Kosek, H. Ševčíková and M. Marek, J. Phys. Chem. **99**, 6889 (1995).

[21] H. Ševčíková, I. Schreiber, and M. Marek, J. Phys. Chem. **100**, 19153 (1996).
[22] J. Lindner, H. Ševčíková, J. Kosek, and M. Marek (unpublished).
[23] B. Vasiev, F. Siegert, and C. Weijer, Phys. Rev. Lett. **78**, 2489 (1997).
[24] J. L. Martiel and A. Goldbeter, Biophys. J. **52**, 807 (1987).
[25] M. Falcke and H. Levine, Phys. Rev. Lett. **80**, 3875 (1998).
[26] J. Lauzeral, J. Halloy, and A. Goldbeter, Proc. Natl. Acad. Sci. U.S.A. **94**, 9153 (1997).
[27] M. Marek and I. Schreiber, *Chaotic Behaviour of Deterministic Dissipative Systems* (Cambridge University Press, Cambridge, 1995).
[28] E. F. Keller and L. A. Segel, J. Theor. Biol. **26**, 399 (1970).
[29] T. Höfer and P. K. Maini, Phys. Rev. E **56**, 2074 (1997).
[30] A. A. Polezhaev, V. Zykov, and S. C. Müller, Phys. Rev. E **58**, 6328 (1998).